ISSN 0511-5728
The West Indian Journal of Engineering
Vol.39, No.1, July 2016, pp.81-89

A Biosensor for Automated Feature Extraction and Non-invasive Cardiovascular Diagnosis Using Photoplethysmography Waveforms

Nalini Gayapersad[a] and Sean Rocke[b,Ψ]

Department of Electrical and Computer Engineering, The University of the West Indies, St. Augustine Campus, Trinidad and Tobago, West Indies;
[a]E-mail: gayapersad.nalini@gmail.com
[b]E-mail: sean.rocke@sta.uwi.edu

[Ψ] *Corresponding Author*

(Received 29 October 2015; Revised 16 April 2016; Accepted4 June 2016)

Abstract: *Indices derived from the morphological features of photoplethysmography waveforms are increasingly being investigated and linked to cardiovascular diseases, and may eventually be used to enhance patient risk assessments. These indices can be retrieved faster than the results for cholesterol tests (i.e., which are typically required for many risk assessments), are non-invasive, and may be less costly. This paper presents an overview of the development of a non-invasive, continuous, compact and portable device used to acquire the cardiovascular data necessary for assessment and diagnosis in real-time. Typically these indices are not evaluated in real-time, but are instead assessed offline and manually, once the waveform is retrieved. The system presented performs real-time, automatic feature extraction for cardiovascular diagnosis by identifying the 'a', 'b' and 'e' waves derived from the second derivative of the photoplethysmogram waveform, followed by calculating indices associated with these waves. Results demonstrate the feasibility and utility of such a system as an enabler of personalised cardiovascular care systems. Results from demonstrative tests with test subjects are comparable to those in the literature. This paper also offers valuable insights into the challenges in deploying automated, non-invasive, continuous monitoring systems for extraction of cardiovascular health indicators beyond heart rate and blood pressure.*

Keywords: *Automatic feature extraction, biosensor, cardiovascular diagnosis, medical device, photoplethysmography*

1. Introduction

Cardiovascular disease (CVD) is one of four main types of non-communicable diseases (NCDs) which are the leading causes of death globally (WHO, 2014). In a comparison of NCDs that are categorised as leading causes of death in the years 2000 and 2012, heart disease contributed significantly to the number of deaths per year (WHO 2014). There was an alarming increase of deaths from CVDs, such as ischaemic heart disease, hypertensive heart disease and stroke, from 12.5 million in 2000 to 15.2 million in 2012 (WHO 2014). The Caribbean is one of the most affected regions of the Americas, as chronic diseases are now the main cause of early death. In 2008, the Caribbean region was ranked the third in the number of deaths from NCDs compared to the total number of deaths in that region (THCC, 2014).

Given the impact upon the region, it is necessary to reduce the incidence of CVDs and healthcare costs. A key strategic intervention is predicting the likelihood of developing CVDs and associated complications. To assess a patient's risk of developing a CVD, multivariable risk prediction approaches have been developed which incorporate risk factors such as age, sex, and blood pressure ~~etc.~~ (D'Agostino et al., 2008). These assessments, as well as monitoring the disease, can be important to reversing the epidemic which has led to a rise in deaths and disabilities from NCDs. Emerging evidence has shown that clinical decisions based on CVD risk assessment, which includes prescribing the relevant drugs, has led to improved management of CVD risks. For example, initial risk assessment and targeted treatment can lead to a reduction in the risk of CVDs such as cardiovascular heart disease (CHD) (Heart Foundation, 2015).

Photoplethysmography (PPG) is an optical measurement technique that can be used to capture cardiovascular data. Indices calculated from the physiological features identified from the PPG waveform are being correlated with the risk of CHD in individuals (Elgendi, 2012). Other risk assessments, such as the popular Framingham risk model and other models discussed in Bitton and Gaziano (2010), typically use age, gender, cholesterol and systolic blood pressure to calculate the risk score (D'Agostino et al., 2008). To obtain a cholesterol reading a sample of blood is required from the patient, whereas the PPG waveform, from which the indices are calculated, is retrieved non-invasively (Lai and Insoo, 2015). In addition to using non-invasive measurements, PPG devices can be used to continuously monitor patients and provide these indices,

shortly after measurement. This is in contrast to typical assessments, for which there are long delays in obtaining the results, for example the cholesterol test (Mayo Clinic 2015).

Consequently, using PPG-based devices with appropriate signal processing techniques to estimate alternative risk indices, such as those proposed in Elgendi (2012), would also increase the frequency of risk evaluations for CHDs. This facilitates increased personalised and data-driven treatment for persons who may have or may develop CVDs. Furthermore, the ability to track progression of CVDs would help determine the degree to which intervention such as lifestyle changes or medication are lowering the impact CHDs.

PPG-based devices offer several advantages in addition to low manufacturing costs. They can also be wearable devices, such as wrist wearable units (e.g., watches) (Ahanathapillai et al., 2015), and they can be integrated with mobile devices, such as smart phones (Lai and Insoo, 2015). Wearable devices are becoming more popular since this increases the ability for patient self-monitoring (Lewy, 2015). This can save on the cost associated with tests required by the Framingham model as well as the inconvenience of going to the laboratories or healthcare facilities to have tests done (Mansor et al., 2013). Such devices are also advantageous for providing healthcare professionals with important patient data in cases where access is a challenge, such as in remote or under-resourced communities, or even between patient visits or routine follow-up.

PPG waveforms offer tremendous potential for determining key health indicators. For example, there has been considerable work on developing portable PPG-based devices which capture the PPG waveform for estimating heart rate or blood pressure automatically, for example finger oximeters (DMG, 2015). These waveforms have also been used to automatically estimate blood oxygen content (Covidien, 2014). However, further automatic feature extraction required for cardiovascular diagnosis is limited. Either the waveforms are not accessible to the end user, or if they are then the indices are calculated offline by visual inspection of the waveform to manually identify the relevant morphological features (Gonzalez, 2008).

This paper builds on the existing work in PPG-based diagnosis and presents the development of a compact, portable device for automatic feature extraction of relevant cardiovascular metrics for cardiovascular assessment and diagnosis in real-time. The development of this device is aimed at making cardiovascular diagnosis more affordable, and accessible, particularly to those in resource-constrained or remote locations. To the best of the authors' knowledge such functionality has not been realised in current commercial devices, and therefore a gap currently exists. Given the incidence of cardiovascular diseases in the Caribbean and globally, this device has tremendous potential for integration into a personalised health care strategy for the diagnosis and treatment of cardiovascular diseases.

The paper is organised as follows. Section 2 provides a brief introduction to PPG, and describes the technique by which the PPG waveform is retrieved. The indices developed from the PPG waveform, some of which will be derived by the system, are discussed in Section 3. Section 4 presents the technical system which retrieves the PPG waveform continuously and non-invasively; acquires the necessary physiological features; and calculates the values of the indices in real-time. The method by which the system is tested is described in Section 5. An analysis of the results retrieved by the system is discussed in Section 6. Recommendations for future works based on issues discussed in Section 6 are presented in Section 7, followed by concluding statements in Section 8.

2. Photoplethysmography

For the PPG technique, the volume of pulsating blood (i.e., the blood volume pulse – BVP) at a part of the body is estimated by detecting the amount of reflected or transmitted light when a light source illuminates the measurement site. Typically the light source is a light emitting diode (LED) and the detector is a photodiode or phototransistor. For both reflection type and transmission type of the PPG measurement techniques, the principles of light absorption, light transmission and light dispersion determine the sensed PPG waveform. For both techniques a decreased volume of blood in the area in which the sensor is placed results in an increase in the intensity of the received light by the photodetector. Increased blood volumes result in decreased received light intensity.

Since PPG-based techniques are optical in nature, it is expected that performance would depend upon the properties of chosen wavelengths for system operation. It has been observed that the dominant absorption peak corresponding to red blood cells is in the blue region of the spectrum, followed by the green-yellow region (between 500 and 600 nm) (Tamura et al., 2014). Red wavelengths could be used for retrieving the PPG waveform since they sufficiently penetrate various measurement sites (Elgendi, 2012). However, infrared (IR) or near-IR light have longer wavelengths than the red, green and blue (RGB) wavelengths and hence are better for measurement of deep-tissue blood flow (Tamura et al., 2014). Wavelengths shorter than that of the RGB wavelengths are strongly absorbed by melanin. In recent literature green light is becoming increasingly popular, although it is less penetrating than IR, due to its higher signal to noise ratio compared to IR wavelengths (Tamura et al., 2014).

PPG waveforms can be separated into a slowly-varying baseline (referred to as the DC component in the literature) and a pulsatile component (referred to as the

AC component in the literature). The DC component arises from lower frequency biological signals including those due to respiration, thermoregulation and the sympathetic nervous system. The AC component arises due to changes in the blood volume at the measurement site with each heartbeat. Figure 1 illustrates an example of a PPG waveform.

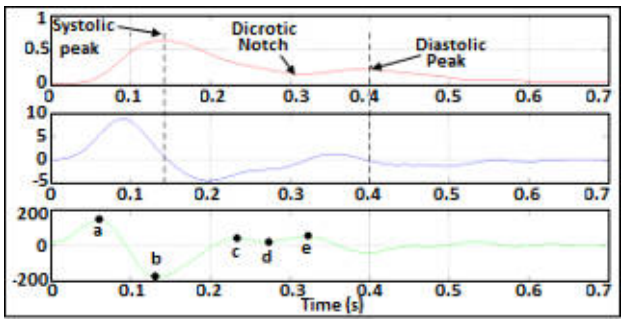

Figure 1. Example PPG waveform (upper figure) with critical points of the second derivative of the PPG waveform (lower figure)

The AC component is superimposed onto the DC component and contains the information needed for cardiovascular diagnosis. The AC component of the PPG waveform has 2 peaks and a "notch" or a point of inflection in the downslope (Laucevičius et al., 2004). The notch, also referred to as the dicrotic notch, corresponds to the closure of the aortic valve at the end of systole which causes momentary increase in blood volume of the arteries (Elgendi, 2012). The systolic peak corresponds to the heart muscle contracting and pushing blood through the arteries, whereas the diastolic peak corresponds to the heart muscle resting between beats and refilling with blood (American Heart Association, 2014).

3. Indices derived from PPG waveform

For cardiovascular diagnosis, the critical points of the PPG waveform are found by determining the second derivative of the photoplethysmogram (SDPTG) with respect to time (Elgendi, 2012). This allows for easier and more accurate interpretation of the inflection points (AHA, 2014). Figure 2 illustrates an example of a PPG waveform and the derived SDPTG. Features used from the first derivative of the PPG waveform (middle sub-figure) are not used in this work. The SDPTG is made up of four systolic waves, which are the 'a' to 'd' waves and one diastolic wave, which is the 'e' wave (Elgendi, 2012). The ratios which have been calculated from the critical points of the SDPTG are:

- the b/a ratio - an indicator of arterial stiffness which increases with age and increasing arterial stiffness (Baek et al., 2012);
- the c/a ratio - an indicator of arterial stiffness which decreases with age (Baek et al., 2012);
- the d/a ratio - an indicator of arterial stiffness and vascular tone which both decrease with age (Chowienczyk et al., 1999; University of Maryland Medical Center, 2014);
- the e/a ratio - an indicator of arterial stiffness which decreases with age (Elgendi, 2012);
- the aging index, expressed as ((b - c - d - e)/a or (b - e)/a) – an indicator of vascular aging and arteriosclerotic disease (Elgendi, 2012).

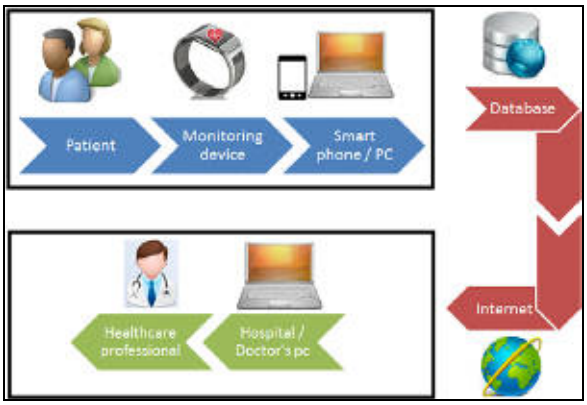

Figure 2. System data flow overview

Although these indices have been the primary focus of the investigation into characterising arterial health, they can be used to investigate other pathologies indicative of CVD, such as the diseases listed in Table 1. However, a full understanding of the diagnostic value of the different features, with respect to the application of the indices to the diseases, is still being researched (Elgendi, 2012).

4. Cardiovascular Monitor Design

The implemented interface allows for data transferred over the internet to be viewed and analysed remotely by a healthcare official, provided the relevant ICT access is available. The implemented measurement system contains a monitoring module, a data collection module, a data analysis module and a user interface. Figure 3 shows the hardware components used in the modules. The monitoring module comprises of the optoelectronic sensor and pre-processing circuitry for amplification and filtration of the received PPG waveform. A microcontroller was used for the data collection module and to communicate to the data analysis module and the user interface. In the data analysis module, the data is further filtered and processed to extract features of the waveform which are analysed. The user interface displays the resultant information, processed in the data analysis module, to the user.

Table 1. Types of Heart Disease (Source: Extracted from WHF (2014)

Type of Heart Disease	Cause	Effect
rheumatic	several attacks of rheumatic fever	damages the heart valves
hypertensive	high blood pressure (BP)	overburdens the heart and blood vessels
ischemic	the narrowing of the coronary arteries	reduces the blood flow to the heart
cerebrovascular	obstructed blood supply to the brain	leads to strokes
inflammatory	toxic or infectious agents	inflammation of the heart muscle

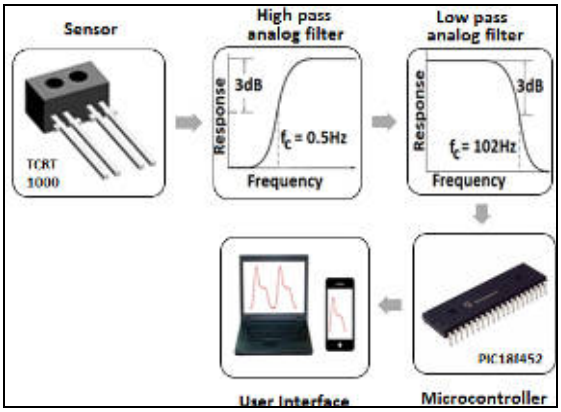

Figure 3. Hardware components utilised for each module

The implemented cardiovascular diagnostic system was intended to be more compact and portable than the PPG diagnostic system developed by Elgendi (2012). And the system discussed in this paper automates the evaluation of the indices discussed in the previous section. The end goal was to enable automatic evaluation of the presence and extent of different heart diseases, as opposed to the typical functionality of current PPG-based devices which primarily focus on blood pressure, heart rate monitoring, and blood oxygen saturation.

The diagnostic system comprises several signal processing stages, as shown in Figure 4. The first stage is the retrieval of the cardiovascular signal using an optoelectronic sensor. The next stage is pre-processing of the PPG signal using analog signal processing to isolate the desired PPG waveforms. The DC component is filtered out of the signal, using a high pass filter with cut-off frequency 0.5Hz, since the AC signal contains the necessary information. Low pass filters are used to aid in identifying key points of the waveform and minimise power line interference without compromising the integrity of the signal. An active analog filter was used to amplify the output of the sensor, and to prevent aliasing during analog-to-digital conversion. Following analog signal processing and analog-to-digital conversion the digitised signal was sent to the microprocessor. The third stage (implemented in the microprocessor) included data transmission and feature extraction.

Figure 4. Signal processing stages of implemented cardiovascular diagnostic system

For this study, feature extraction involved the determination of the 'a', 'b' and 'e' waves, since most of the indices can be calculated by using only these waves. To identify these features a period of the PPG waveform is first extracted and then the systolic peak, the diastolic peak and the dicrotic notch of the PPG waveform are identified. The indices that are subsequently calculated are the b/a, e/a, and (b-e)/a, (i.e., the aging index).

4.1 Feature extraction algorithm

To determine the 'a', 'b' and 'e' waves, the systolic peak, the diastolic peak and the dicrotic notch were extracted. To identify the systolic peak, the diastolic peak and the dicrotic notch it was necessary to extract a period of the waveform. Strictly speaking the waveform is quasiperiodic, but for the measurement interval, the captured sequence of waveforms is assumed to be approximately periodic, which is reasonably assumed in practice (Elgendi, 2012). Following this assumption, each period of the PPG waveform has a:

- prominent positive-going zero-crossing corresponding to the start of the waveform; and
- less pronounced positive-going zero-crossing, corresponding to the dicrotic notch.

Smoothing was used to determine the more prominent positive-going zero-crossing points to find the period between zero-crossings. Upon extraction of the period, the systolic peak and the diastolic peak were identified. Figure 5 illustrates the algorithm for this. The first derivative of the period of the PPG waveform was then used to determine the positive-going zero that corresponded to the dicrotic notch of the PPG signal. To reduce the fluctuations in the amplitude of the first derivative, to clearly identify the positive-going zero-crossing points, smoothing was used. These false zero-crossings were as a result of random fluctuations in the amplitude of the first derivative.

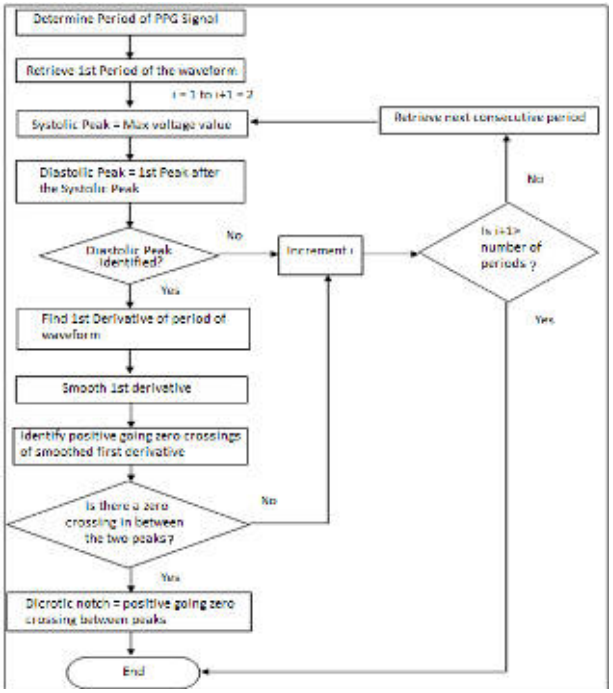

Figure 5. Algorithm to identify systolic peak, diastolic peak and dicrotic notch

If these features could not be identified from the extracted period, which may be as a result of distortion due to motion artefacts, another period from the recorded dataset was used. Once the systolic peak, diastolic peak and dicrotic notch were identified the second derivative was calculated from the unsmoothed first derivative, which was then used in conjunction with the PPG signal to determine the 'a', 'b' and 'e' waves. Figure 6 illustrates the algorithm for this.

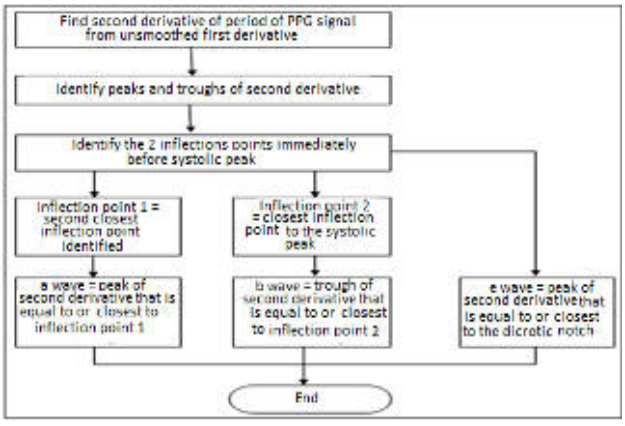

Figure 6. Wave identifying algorithm

5. System Testing

The system's functional requirements were verified in two stages:

- unit testing – testing of each individual module e.g. testing the sensor to ensure a PPG waveform was being retrieved; the microcontroller to ensure that it was accurately retrieving and transmitting the PPG voltages; and the algorithms used for signal processing
- system testing – testing of interconnected modules

For system testing, each test subject was required to remain as motionless as possible, to reduce motion artefact, and the sensor was placed on the measurement site. The PPG waveform was captured, and processed using the automatic feature extraction approach described and displayed using the user interface which was implemented as a MATLAB executable. Figure 7 shows an example screenshot of the implemented user interface for visualisation of the signal points of interest, as well as to display the automatically-extracted indices.

Following system testing, the system was further evaluated using 10 test subjects. Appropriate permissions were obtained prior to collecting data from test subjects. The medical state/history of each test subject was unknown. The heart rate, gender, age and weight and height for each of the 10 test subjects were recorded before testing. The sensor from the monitoring module was placed on each test subject to observe the PPG waveforms being retrieved. To retrieve the best suited waveform, the sensor was positioned on the left wrist. Each subject was required to remain as motionless as possible to reduce disturbances due to motion artefacts of captured waveforms. Captured data was used to extract the features and determine indices demonstrating the required functionality of the system.

6. Results and Analysis

Table 2 is a compilation of the information recorded from the test subjects. In addition to functional testing, the system performance has to be assessed to provide a baseline for future work on enhancements to the system.

Of prime importance at this stage was the error performance of the implemented system. Currently, there are no available gold standard devices which extract the features and indices which can be used for comparison. Therefore visual inspection and waveform annotation by an expert provided a reliable method for comparison to the automatically-extracted features for error analysis. This is the currently accepted approach in the literature (see Elgendi 2012).

Table 2. Summary of characteristics parameters of test subjects

Number of Subjects	10
Male/ Female	5/5
Age range (years)	20-53
Heart rate range (bpm)	70 –111
Weight range (kg)	54.4-90.7
Height range (m)	1.6- 1.8
Body mass index range (kg/ m^2)	19.0 - 27.9

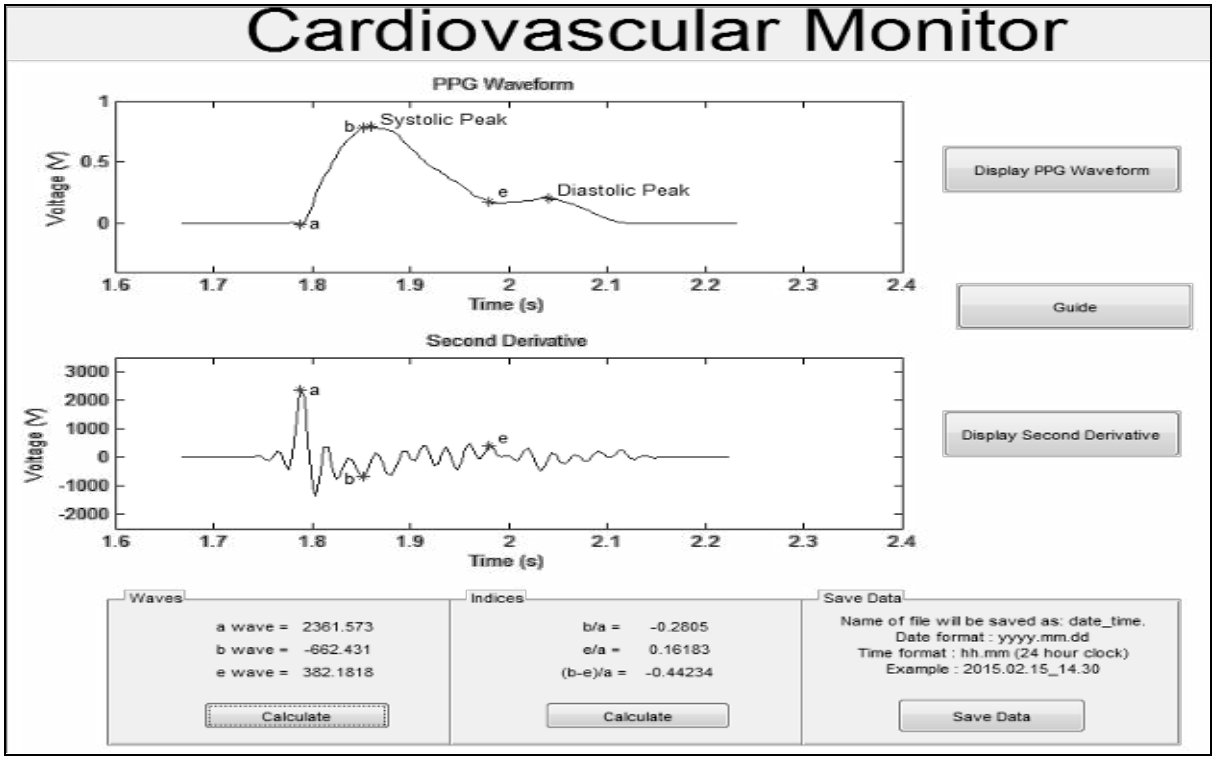

Figure 7. Example screenshot of user interface for cardiovascular monitor

Figures 8, 9 and 10 present the error graphs for each index, comparing the indices derived from automatically-extracted waves to the indices derived from expert visual inspection of the waves for all test subjects. While in general, as seen from the plots, there was a small deviation of the automatically-derived values from the values identified by visual inspection for the 'a' and 'b' waves for both genders, the 'e' wave sometimes deviated significantly.

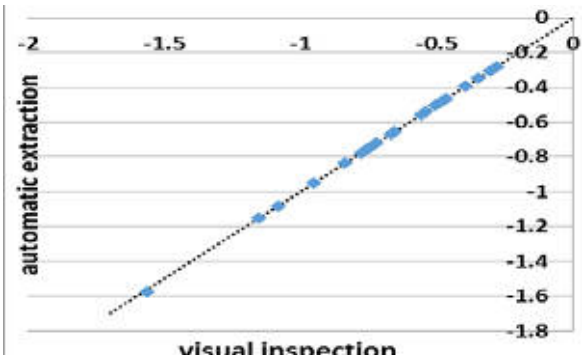

Figure 8. Comparison of automatically extracted b/a index to expertly visually extracted b/a index

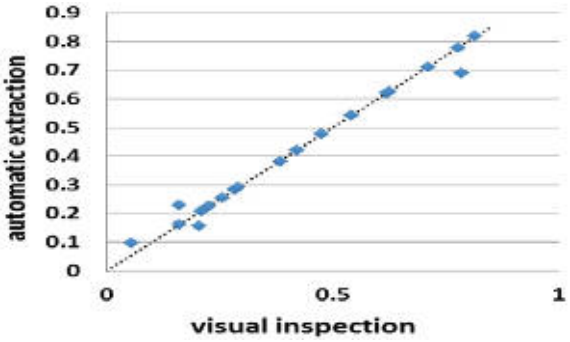

Figure 9. Comparison of automatically extracted e/a index to expertly visually extracted e/a index

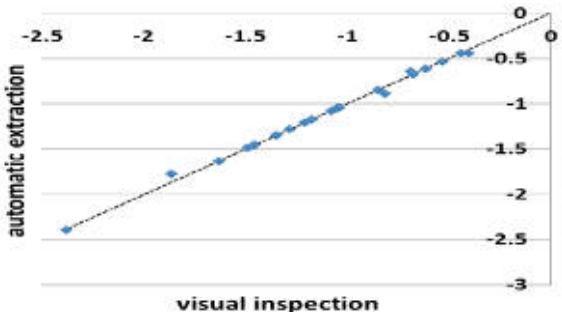

Figure 10. Comparison of automatically extracted (b-e)/a index to expertly visually extracted (b-e)/a index

This heavily impacted the e/a index and the aging index as seen in Table 3 since the mean square errors (MSE) for both were higher than that of the b/a index. However the MSE for all were small which suggests that the implemented algorithms were fairly accurate. Despite measurement precautions, errors in identifying the waves could have been due to motion artefacts.

Table 3. Mean Square Error for each index

Index	MSE
b/a	0.000008
e/a	0.000680
(b-e)/a	0.000698

The system was further validated through comparison of the relationships between the variables BMI, weight, height and age with each index. This was done by measuring the correlation of each index with the listed parameters using the Spearman's Rank Correlation (SRC). The results in Table 4, where correlated to both the automatically-derived indices as well as to the expert-derived values are given. The following is the ranges for the types of correlation that were used to analyse the data (Laerd Statistics, 2016):

- high correlation: 0.5 to 1.0 or - 0.5 to -1.0
- medium correlation: 0.3 to 0.5 or -0.3 to -0.5
- low correlation: 0.1 to 0.3 or -0.1 to -0.3

Further validation involved comparing results to that in related work. The obtained results were similar to those reported in the literature. For instance, it was observed that BMI and age have medium to high correlation with these indices, while weight had a medium correlation and height had a low correlation. The BMI is an index that is calculated using height and weight and is used as a measure of obesity. Since obesity is a risk factor for heart diseases (British Heart Foundation, 2014) then it should be expected that as the BMI increases, the risk of heart disease should generally increase (Pilt et al., 2014).

In a study conducted by Chen et al., (2013) a high BMI (> 25) was associated with CHD especially for individuals below the age of 53. From this small scale study, it was observed that test subjects with higher BMIs (looking at BMI independent of other factors) generally had higher b/a and aging indices (more positive) and a decreased e/a index is associated with heart diseases such as atherosclerosis. According to the Texas Heart Institute (2014) as age increases the risk of developing CHD increases as the heart's walls may thicken and arteries may stiffen and harden. This was borne out by the data as age had a medium to high correlation which the indices.

Although height and weight are both contributing factors to BMI, which had a high correlation to the indices, they have medium to low correlation with the indices. Since weight is a large contributing factor to obesity, the correlation of the indices with weight was expected to be similar to that for BMI. This trend was observed, as seen in Table 4.

Using similar reasoning, since height contributes less to obesity a lower correlation was expected between height and the indices. Table 4 also highlights this. The results are further supported by the main trends observed in the literature (Chowienczyk et al., 1999; Elgendi, 2012; Baek et al., 2012; University of Maryland Medical Center, 2014). Thus, although there were some observable measurement errors (refer to Figures 9-11), the indices followed trends discussed in past literature: the b/a and (b-e)/a indices generally increased with age, i.e. became more positive, since the values for these indices are negative; whereas the e/a index generally decreased with age.

Table 4. Spearman's Rank Correlation for the relationship between the indices and BMI, weight, height, age and each other

Degree of Correlation	Relationship	Spearman's rank correlation coefficient	
		Automatically Extracted Value	Value from Visual Inspection
High	b/a index vs aging index	0.92	0.92
	b/a index vs age	0.88	0.88
	aging index vs age	0.86	0.86
	e/a index vs aging index	-0.83	-0.83
	e/a index vs age	-0.77	-0.77
	aging index vs BMI	0.76	0.76
	b/a index vs BMI	0.71	0.71
	b/a index vs e/a index	-0.70	-0.70
	e/a index vs BMI	-0.62	-0.62
Medium	e/a index vs height	0.41	0.41
	aging index vs weight	0.41	0.41
	b/a index vs weight	0.34	0.34
Low	b/a index vs height	-0.25	-0.25
	aging index vs height	-0.24	-0.24
	e/a index vs weight	-0.21	-0.21

7. Conclusion and future work

An overview of the development of a continuous, non-invasive cardiovascular monitoring device for the real-time extraction of cardiovascular features was presented. The monitoring device automatically identified cardiovascular features which were used to calculate indices that would possibly provide information about the cardiovascular health of an individual. Initial results demonstrate the functionality of this system, and corroborate results presented in the literature. This system may therefore form the basis from which remote monitoring systems can be developed to increase self-monitoring.

The proposed system is in line with increasing research into the use of wireless sensors for monitoring individual medical data continuously, outside of traditional settings (e.g., clinic, doctor's office, hospital). Such technology would equip individual patients with better health monitoring capabilities, while also providing healthcare researchers and service providers with valuable data for enhancing diagnosis, treatment and prevention strategies.

Visual inspection was the reference for the derived values, since there was no commercially available solution that could be used to automatically extract 'a'-'e' waves or annotate PPG-waveforms with the 'a'-'e' waves for measurement and comparison to the implemented system. The accuracy of the system can only be gauged from a "gold standard" device. For further work the system will be enhanced to fill this gap.

Additionally, there are no standard measurement protocols currently available to account for measurement variability due to posture and positioning of test subjects. This is extremely important, given the impact of motion artefacts in PPG-based signal acquisition and processing and considering that PPG-based devices, especially wearable devices, are susceptible to motion artefacts (Lai, 2015; Kim and Yoo, 2006). Thus future work will include the implementation of low-computational cost motion artefact compensation algorithms to further improve the accuracy of the measurements.

Finally, while the general functionality and small-scale performance of the device was investigated, the device needs to be further tested in a wider scope of scenarios, using a wider range of test subjects.

References:

Ahanathapillai, V., Amor, J.D, Goodwin, Z and James, C.J (2015), "Preliminary study on activity monitoring using an android smart-watch", *Healthcare Technology Letters*, Vol.2, No.1, February, pp 34-39.

AHA (2014), *About High Blood Pressure*, American Heart Association, Accessed 23 June 2014 from: http://www.heart.org/HEARTORG/Conditions/HighBloodPressure/AboutHighBloodPressure/Understanding-Blood-Pressure-Readings_UCM_301764_Article.jsp

Baek, H.J., Kim, J.S., Kim, Y.S., Lee, H.B. and Park, K.S. (2007), "Second derivative of photoplethysmography for estimating vascular aging", *Proceedings of the 6th International Special Topic Conference on Information Technology Applications in Biomedicine*, Tokyo, November, pp 70-72.

BHF (2014), *British Heart Federation*, Accessed 3 July 2014, from: http://www.bhf.org.uk/heart-health/conditions/cardiovascular-disease.aspx

Bitton, A. and Thomas, G (2010), "The Framingham Heart Study's impact on global risk assessment", *Progress in Cardiovascular Diseases*, Vol. 53, No. 1, July, pp. 68-78.

Chen, Y., Copeland, W.K, Vedanthan, R., Grant, E., Lee, J. E, Gu, D. et al. (2013), "Association between body mass index and cardiovascular disease mortality in east Asians and south Asians", *Asia Cohort Consortium*, October, pp. 347-446.

Chowienczyk, P.J., Kelly, R.P, MacCallum, H., Millasseau, S.C., Andersson, T.L.G., Gosling, R.G., Ritter, J.M., and Änggård, E.E. (1999), "Photoplethysmographic assessment of pulse wave reflection: blunted response to endothelium-dependent beta2-adrenergic vasodilation in type II diabetes mellitus", *Journal of the American College of Cardiology*, Vol.34, No.7, December, pp. 2007-2014.

Covidien (2015), *Covidien*, Accessed 10 October 2015, from: http://www.covidien.com/rms/products/pulse-oximetry/nellcor-spo2-reusable-sensors

DMG (2015), *Dolphin Medical Group*, Accessed 10 October 2015, from: http://www.viamed.co.uk/eng/Uploads/OEM%20modules%2000192601.pdf

D'Agostino, R B., Vasan, R.S., Pencina, M.J., Wolf, P.A., Cobain, M., Massaro, J.M. and Kannel, W.B. (2008), "General cardiovascular risk profile for use in primary care the Framingham Heart Study", *Circulation*, Vol.117, No.6, February, pp.743-753.

Gonzalez, R., Manzo, A., Delgado, J., Padilla, J. M., Trenor, B. and Saiz, J. (2008), "A computer based photoplethysmographic vascular analyser through derivatives", *Computers in Cardiology*, September, pp.177-180.

Heart Foundation (2015), *Heart Foundation*, Accessed 25 July 2015, from: http://www.heartfoundation.org.au/SiteCollectionDocuments/guidelines-Absolute-risk.pdf

Elgendi, M. (2012), "On the analysis of fingertip photoplethysmogram signals", *Current Cardiology Review*, Vol.8, No.1, February, pp 14-25.

Kim, B.S., and Yoo, S.K. (2006), "Motion artifact reduction in photoplethysmography using independent component analysis", *Biomedical Engineering, IEEE Transactions*, Vol.53, No.3, March, pp.566-568.

Laerd Statistics (2016), *Laerd Statistics*, Accessed 28 April 2016, from: https://statistics.laerd.com/statistical-guides/pearson-correlation-coefficient-statistical-guide.php

Lai, P. and Insoo K. (2015), "Lightweight wrist photoplethysmography for heavy exercise: motion robust heart rate monitoring algorithm", *Healthcare Technology Letters*, Vol.2, No. 1, February, pp. 6-11.

Laucevičius, A., Ryliškyte, L., Petrulioniene, Ž., Kovaite, M. and Misonis, N., (2004), "First experience with salbutamol–induced changes in the photoplethysmographic digital volume pulse", *Seminars in Cardiology*, No. 2, June, pp. 83-90.

Lewy, H (2015), "Wearable technologies – Future challenges for implementation in healthcare services", *Healthcare Technology Letters*, Vol. 2, No. 1, February, pp. 2-5.

Mansor, H., Helmy, M., Shukor, A., Meskam, S.S., Rusli, N.Q.A.M., and Zamery, N.S. (2013), "Body temperature measurement for remote health monitoring system", *Proceedings of 2013 IEEE International Conference on Smart*

Instrumentation, Measurement and Applications (ICSIMA), Kuala Lumpur, November, pp. 1-5.

Mayo Clinic (2015), *Mayo Clinic*, Accessed 25 July 2015, from: http://www.mayoclinic.org/tests-procedures/cholesterol-test/basics/what-you-can-expect/prc-20013282

Pilt, K., Meigas, K., Ferenets, R., Temitski, K., and Viigimaa, M. (2014), "Photoplethysmographic signal waveform index for detection of increased arterial stiffness", *Physiological Measurement*, Vol.35, No. 10, October, pp 2027– 2035.

Rebel, A., Rice, M.A., and Fahy, B.G. (2012), "The accuracy of point-of-care glucose measurements", *Journal of Diabetes Science and Technology*, Vol. 6, No.2, March, pp. 396-411.

Tamura, T., Maeda, Y., Sekine, M. and Yoshida, M. (2014), "Wearable Photoplethysmographic Sensors: Past and Present", *Electronics*, Vol. 3, February, pp. 282-302.

THI (2014), *Texas Heart Institute*, Accessed 3 July 2014, from: http://www.texasheart.org/HIC/Topics/HSmart/riskfact.cfm

THCC (2014), The Healthy Caribbean Coalition, Accessed 30 June 2014, from: http://www.healthycaribbean.org/UNHLM-HCC/Caribbean-NCDs-Fact-sheet.pdf

UMMC (2014), *The University of Maryland Medical Center*, Accessed 28 June 2014, from: //umm.edu/health/medical/altmed/condition/atherosclerosis#ixzz35zAAnqKX

Wentholt, I.M., Hoekstra, J.B., and DeVries, J.H. (2006), "A critical appraisal of the continuous glucose–error grid analysis", *Diabetes Care*, Vol.29, No.8, August, pp.1805-1811.

WHO (2014a), *World Health Organisation*, Accessed 29 June 2014, from: http://whqlibdoc.who.int/publications/2011/9789240686458_eng.pdf?ua=1

WHO (2014b), *Factsheets*, World Health Organisation, Accessed from: http://www.who.int/mediacentre/factsheets/fs310/en/

WHF (2014), *Cardiovascular Health*, World Heart Federation, Accessed 3 July 2014, from: http://www.world-heart-federation.org/cardiovascular-health/heart-disease/different-heart-diseases/

Authors' Biographical Notes:

Nalini Gayapersad *received her B.Sc. degree in Electrical and Computer Engineering, with concentrations in Energy Systems and Control Systems, at The University of the West Indies, St. Augustine. Her current work involves biosensor research and development, and signal processing algorithms for medical diagnostic systems to be used for personalised health monitoring.*

Sean Rocke *received his BSc in Electrical & Computer Engineering from The University of the West Indies in 2002, his Masters in Communications Management and Operational Communications from Coventry University in 2004, and his Ph.D. in Electrical & Computer Engineering from Worcester Polytechnic Institute in 2013. His areas of interest include signal processing and optimisation techniques relating to wireless communications management applications, biosensor development and biological data mining, as well as emergency communication systems.*

■